

***CPR1*: A Gene Encoding a Putative Signal Peptidase That Functions in Pathogenicity of *Colletotrichum graminicola* to Maize**

M. R. Thon, E. M. Nuckles, J. E. Takach, and L. J. Vaillancourt

Department of Plant Pathology, S-305 Agricultural Sciences Center-North, University of Kentucky, Lexington 40546-0091, U.S.A.

Submitted 10 September 2001. Accepted 29 October 2001

Colletotrichum graminicola causes anthracnose leaf blight and stalk rot of maize. We used restriction-enzyme mediated insertional (REMI) mutagenesis to identify a gene in this fungus that is required for pathogenicity to both stalks and leaves. The predicted polypeptide encoded by this gene, which we have named *CPR1*, is similar to a family of proteins that comprise one subunit of the eukaryotic microsomal signal peptidase. The nonpathogenic *CPR1* REMI mutant contains a plasmid integration in the 3' untranslated region of the gene, 19 bp downstream from the stop codon. The result is a significant reduction in transcript levels in comparison to the wild type, perhaps as a result of increased transcript instability. We were unable to knock out the *CPR1* gene, and it may be essential for viability. Microscopic examination of the REMI mutant on maize leaves revealed that it is fully capable of penetrating and colonizing host cells during the initial, biotrophic phases of the disease interaction but, unlike the wild type, it appears to be unable to switch to a necrotrophic mode of growth. We suggest that the *CPR1* REMI mutant may be unable to secrete sufficient quantities of degradative enzymes to support that transition. The *CPR1* REMI mutant provides us with a useful tool for future studies of the role of fungal protein transport in this important stalk rot disease of maize.

Additional keyword: signal peptidase complex.

Colletotrichum graminicola (Cesati) Wilson causes anthracnose stalk rot (ASR) and anthracnose leaf blight (ALB) of maize. ASR is the most damaging of the two disease phases and is considered to be one of the most common and economically important of the fungal stalk rots of maize (Bergstrom and Nicholson 1999; White 1999). Although *C. graminicola* is a ubiquitous pathogen with significant destructive potential, very little is known about fungal characters that are important for pathogenicity or aggressiveness of *C. graminicola* on maize stalks or leaves.

We initiated a restriction enzyme-mediated insertional (REMI) mutagenesis project with the goal of identifying genes that play important roles in establishing or maintaining, or both, pathogenic infections of *C. graminicola* in maize stalks.

Corresponding author: L. J. Vaillancourt; Telephone: +1-859-257-2203; E-mail: vaillan@pop.uky.edu

Current address of M. R. Thon: Fungal Genomics Laboratory, North Carolina State University, Campus Box 7251, Raleigh, NC 27695-7251

Using an in vitro pith infection bioassay, we identified a REMI transformant that was unable to rot maize pith tissue (Thon et al. 2000). This transformant also caused no ALB lesions on the leaves of a maize variety that is highly susceptible to the wild-type fungus. We rescued the DNA flanking the plasmid insertion in the mutant, used it to identify a cosmid from a wild-type genomic library, and discovered that the cosmid complemented the pathogenicity defect in the mutant. This suggested that the cosmid contained a pathogenicity gene that had been disrupted in the REMI mutant. The objective of the work described here was to characterize this gene and to obtain evidence for its role in pathogenicity of *C. graminicola* to maize stalks and leaves.

RESULTS

Growth and development of the nonpathogenic REMI mutant in vitro.

We compared spore germination and appressorial formation in vitro and radial growth rate on various media of the nonpathogenic REMI mutant with its progenitor wild-type strain. There were no differences in either spore germination or appressorial formation between the two strains (data not shown). When compared with the wild type, there were small but statistically significant reductions in the growth of the mutant after 7 days on complete nutrient medium, on minimal medium, and on nutrient medium containing pectin and polygalacturonic acid as the carbon sources (Fig. 1).

Growth and development of the nonpathogenic mutant in vivo.

Leaves of the ALB-susceptible maize inbred Mo940, inoculated with conidia from either the wild type or the REMI mutant, were examined microscopically at 24, 48, and 72 h after inoculation. The mutant and the wild type both germinated and formed normal-appearing appressoria within 24 h after inoculation (data not shown). At 48 h, both the mutant and the wild type had penetrated the host epidermis and produced primary infection hyphae, some of which had progressed beyond the initially infected epidermal cells into the mesophyll cells (data not shown). There was no obvious distinction between the REMI mutant and the wild-type strain up to 48 h after inoculation. At 72 h, however, a dramatic difference was evident between the mutant and the wild type. The wild type had entered a necrotrophic phase of growth, and an extensive network of secondary mycelia was seen ramifying throughout the host tissue (Fig. 2A). There was significant host-tissue degradation and necrosis, including death of many cells that had not been invaded by mycelium, and small lesions had become visible at

a macroscopic level. In contrast, the mutant at 72 h after inoculation had colonized a limited number of cells, had not produced secondary mycelia, and did not appear to be causing extensive tissue damage (Fig. 2B). Most of the host cells containing the fungus remained alive and apparently well. We have monitored leaves infected with the REMI mutant up to 2 weeks after inoculation (when they begin to undergo natural senescence), and these leaves never develop macroscopic anthracnose lesions. A more detailed microscopic analysis of infection of susceptible tissues by the mutant will be the subject of a future report.

We reported previously that the REMI mutant strain was equivalent to the nonpathogenic control when it was inoculated into stalks of the corn inbred Mp305 in vivo (Thon et al. 2000). Mp305 is reported to be moderately resistant to ASR (Toman and White 1993), and so in this experiment, we also tested pathogenicity of the REMI mutant in vivo to stalks of a second inbred (OH51A) that is susceptible to ASR in the field (R. Pratt, personal communication). The area of rotted, discolored pith tissue caused by the mutant in vivo on both stalk types was significantly smaller than that caused by the wild-type strain (Fig. 3). On the Mp305 line, the rotted area caused by the mutant was not significantly different from that caused by the nonpathogenic negative control. In the OH51A inbred, the extent of the rot caused by the mutant was slightly greater than that caused by the nonpathogenic control, and this difference was statistically significant.

Cloning and sequencing of the *C. graminicola* pathogenicity gene *CPR1*.

The original cosmid that complemented the nonpathogenic REMI mutant was 50 kb in size. We identified a 3.6-kb *SmaI/EcoRV* fragment of the cosmid that hybridized to the genomic DNA flanking the REMI integration site that had been rescued from the mutant (Fig. 4A). This 3.6-kb fragment was subcloned into pUC18, and the entire plasmid insert was sequenced in both directions (GenBank accession number AF263837). Analysis of the flanking DNA rescued from the mutant had already shown that two copies of the REMI plasmid had integrated into an *EcoRI* restriction recognition site and that there had been no deletion of genomic DNA during the integration (Thon et al. 2000). Sequencing of the 3.6-kb fragment verified this and confirmed the presence of an open reading frame (ORF) that terminates 19 bp upstream of the *EcoRI* REMI integration site. A part of the sequence, including this ORF, is shown in Figure 5. The ORF is predicted to encode a polypeptide of 230 amino acids with a calculated molecular weight of 25.6 kDa and an estimated pI of 9.95. We named this ORF *CPR1*, for *Colletotrichum* pathogenicity related gene 1.

Comparison of the predicted *CPR1* protein sequence to the GenBank database using the BLASTP algorithm (Altschul et al. 1990) produced a significant match to a *Saccharomyces cerevisiae* protein called Spc3p ($E = 2e-12$) (Fig. 6). Spc3p is an essential component of the yeast signal peptidase complex (SPC) (Fang et al., 1997; Meyer and Hartmann 1997). Matches were also found to homologous signal peptidase sequences from *Canis familiaris* ($E = 7e-8$) and *Gallus gallus* ($E = 1e-6$). Other matches were found to several hypothetical proteins identified from genome sequencing projects. Most of these had been classified as probable signal peptidases based on their similarity to either Spc3p or to the canine signal peptidase protein, SPC22/23, or both. They included sequences from *Schizosaccharomyces pombe* ($E = 1e-10$); *Homo sapiens* ($E = 7e-8$); *Arabidopsis thaliana* ($E = 1e-8$); *Mus musculus* ($E = 4e-7$); *Caenorhabditis elegans* ($E = 4e-7$) and *Drosophila melanogaster* ($E = 5e-6$). A TBLASTN search of the recently released

Neurospora crassa genome sequence (assembly version 1, available on-line from the *Neurospora* Sequencing Project, Whitehead Institute/MIT Center for Genome Research) resulted in one highly significant match ($E = 3e-84$) to a sequence on contig 1.627 that has no known function. We found that this region contains an ORF that encodes a predicted protein with a very high degree of similarity to *CPR1* (Fig. 6).

The neural net and the hidden Markov model methods of Nielsen and associates (1997, 1998) for predicting signal peptides and signal peptide cleavage sites both indicated that *CPR1* does contain a signal peptide. However, neither model predicted a cleavage site, suggesting that the signal peptide serves as a signal anchor (Nielsen et al. 1997). Analysis of the predicted *CPR1* protein using the method of Sonnhammer and associates (1998) for identifying transmembrane helices indicated that the protein contains a helical transmembrane domain that comprises amino acids 12 to 34 (Fig. 5).

Analysis of the region upstream of the *CPR1* ORF revealed two potential transcription start sites (Ballance 1986; Gurr et al. 1987) (Fig. 5). One is located at position -4 relative to the presumed translation initiation site, while the other is at position -113. The first ATG in the *CPR1* ORF is presumed to be the translation start site. It is in a nucleotide context that is consistent with the Kozak consensus sequence (ACCATGG) for sites of translation initiation (Kozak 1986). A second ATG occurs in the same reading frame 9 bp downstream from the first. Its nucleotide context is also consistent with a functional start site, and so it could serve as an alternative translation initiation point. Conserved intron splice sites and a consensus lariat sequence (Ballance 1986; Gurr et al. 1987) indicate that the *CPR1* ORF contains one intron (Fig. 5). A near-consensus polyadenylation signal, AATAAT (the consensus sequence is AATAAAA [Gurr et al. 1987]) is found 143 bp downstream of the stop codon.

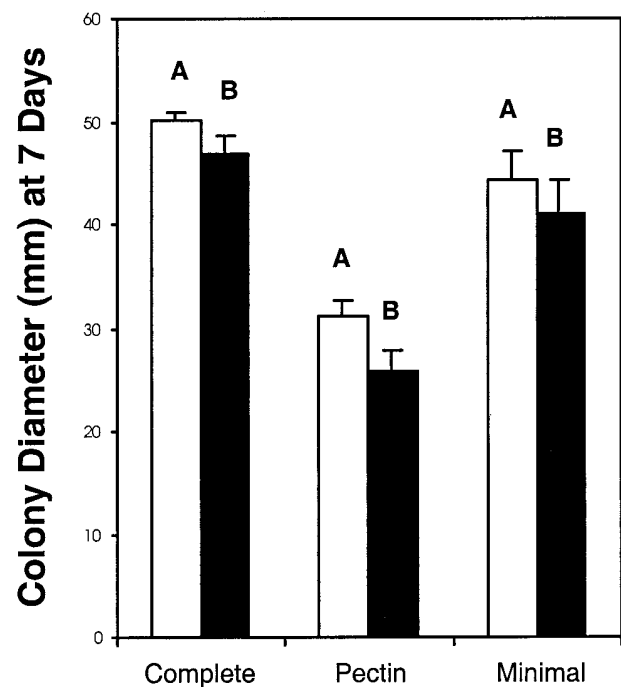


Fig. 1. Comparison of radial growth rates on three different media of the wild-type strain (white bars) and the *CPR1* restriction-enzyme mediated insertional mutant strain (black bars). Measurements were made 7 days after point inoculation of the culture plates. For each medium, bars with different letters were significantly different at $\alpha = 0.5$, calculated using a student's t test.

Analysis of the 3.6-kb subclone containing *CPR1*.

The sequence of the entire 3.6-kb subclone that contained *CPR1* was used to conduct a TBLASTN search against the GenBank sequence database. With the exception of *CPR1* itself, no significant matches were detected. The 3.6-kb sequence was also analyzed by using three different gene-finding algorithms: GENSCAN, trained on vertebrate sequences (Burge and Karlin 1997); FGENES, which was developed using a database of human genes (available on-line from The Sanger Center's Computational Genomics Group); and a version of FGENESH trained on *N. crassa* sequences (available on-line from Softberry, Inc.). GENSCAN and FGENESH both predicted the same *CPR1* gene sequence that we had already derived from our manual analysis. FGENES predicted the same first exon of *CPR1* but produced a different result for the 3' end of the gene. All three programs predicted the existence of a second gene on the 3.6-kb fragment. This putative gene is located upstream of *CPR1* and reads in the opposite direction (Fig. 4A). Each program predicted a different translation start site, but all three versions shared

portions of one exon, and the GENSCAN and FGENESH versions also contained the same terminal exon. BLASTP analyses of the predicted polypeptides encoded by each of the three versions of the putative gene produced no significant matches in any case.

An analysis of codon usage bias using a version of the computer program CodonUse trained on known *C. graminicola* gene sequences (C. Halling, Monsanto Co., St. Louis, MO, U.S.A.) was conducted for the entire 3.6-kb fragment. This revealed that both of the *CPR1* gene exons correspond to regions of significant bias. Although there are other regions displaying significant codon usage bias scattered throughout the rest of the 3.6-kb fragment, all of these are rather short (the largest is only 200 bp), and none correspond to any of the exons in the putative upstream genes predicted by the gene prediction algorithms (data not shown).

One other interesting feature of the 3.6-kb subclone is that it contains a microsatellite sequence consisting of 31 copies of the dinucleotide GA. The sequence is located 1.2 kb upstream of the *CPR1* start codon.

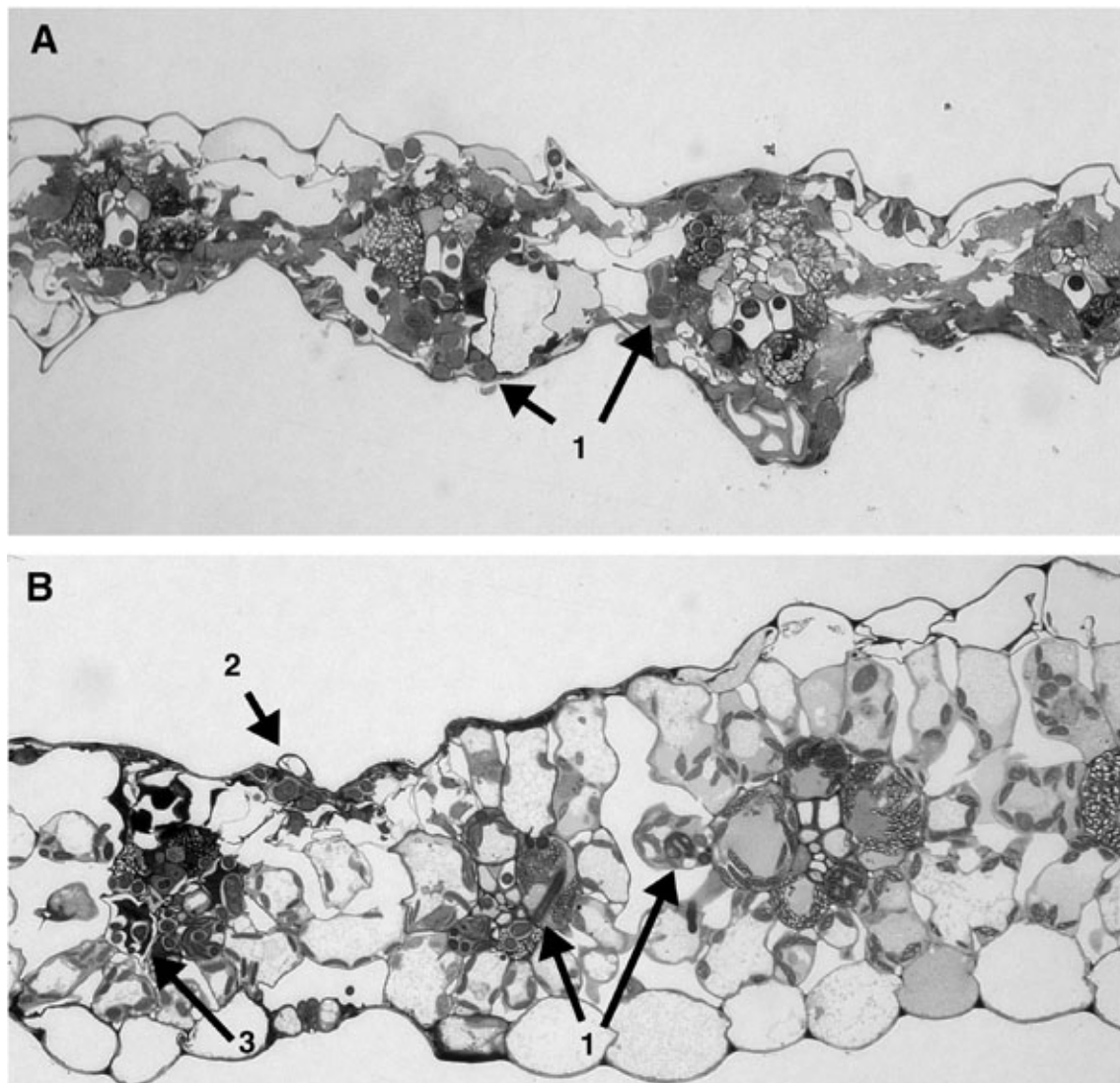


Fig. 2. Light micrographs of sections through maize leaves 72 h after they were inoculated with **A**, conidia of the wild-type strain or **B**, the *CPR1* restriction-enzyme mediated insertional mutant. Note the almost total lack of cellular integrity in the leaf tissue that was inoculated with the wild type. There are numerous fungal hyphae traversing the tissue. A few of these are indicated by arrow 1. In contrast, the tissue inoculated with the *CPR1* mutant is still largely intact. There are fungal hyphae present in some of the mesophyll and bundle sheath cells (arrows 1 and 3), but only a few of these cells have died (arrow 3), and there are fewer hyphae present in the tissue in comparison with the leaf inoculated with the wild type. The remains of an appressorium (arrow 2) can be seen on the surface, and the epidermal cell immediately below it has several hyphae within it. Both sections are at the same magnification, approximately 600x.

Complementation assays.

We reported previously that the 50-kb cosmid containing *CPRI* complemented the nonpathogenic REMI mutant (Thon et al. 2000). The 3.6-kb subclone containing *CPRI* also fully complemented the mutant strain on leaves and on stalks in vi-

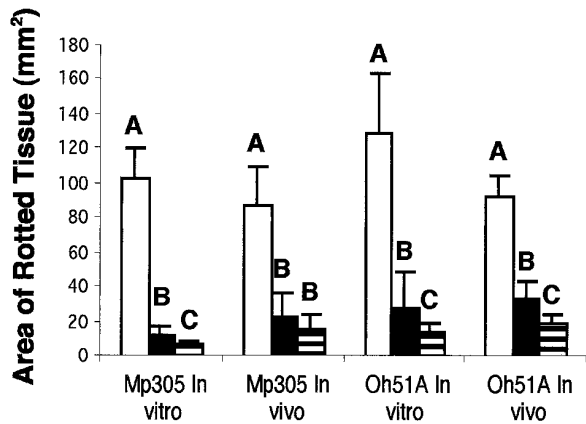


Fig. 3. Degree of rotting of maize pith tissue caused by the wild-type strain (white bars), the *CPRI* restriction-enzyme mediated insertional mutant strain (black bars), and a strain of *Colletotrichum sublineolum* that is nonpathogenic to maize, used as a negative control (striped bars). Two inbreds were tested in these experiments: Mp305, which is considered to be moderately resistant to anthracnose stalk rot (ASR); and Oh51A, which is susceptible to ASR. Analyses were performed on stalk tissue both in vitro using detached stalk pieces, and in vivo on intact plants in the greenhouse. For each treatment, bars with the same letters were not significantly different at $\alpha = 0.5$, calculated using the Waller-Duncan multiple range test.

tro (Fig. 7). Furthermore, transformation with the 3.6-kb subclone complemented the small growth defect of the mutant strain in culture (data not shown).

To analyze the role of the second putative gene that was predicted upstream of *CPRI*, we produced two subclones from the 3.6-kb sequence that contained either *CPRI* or the second putative gene alone (Fig. 4A) and tested them for complementation of the mutant phenotype on leaves and on stalks in vitro. All eleven of the transformants containing the *CPRI* subclone that were tested produced symptoms identical to those produced by the wild-type strain on both leaves and stalks. In contrast, 10 strains containing the subclone encoding the second putative gene produced results that were the same as those resulting from inoculation with the nonpathogenic REMI mutant (data not shown). This result confirms that it is *CPRI* and not the putative second gene on the 3.6-kb fragment that is responsible for the pathogenicity phenotype of the REMI mutant.

Gene disruption.

To further test the function of the *CPRI* gene, we developed a gene disruption construct using an 8-kb *PstI* subclone of the 50-kb cosmid that contained the *CPRI* gene (Fig. 4). The undisturbed 8-kb subclone fully complemented the mutant strain on leaves and on stalks in vitro and in vivo (data not shown). The rationale for using the 8-kb clone for the disruption experiments instead of the 3.6-kb subclone was to increase the rate of homologous integration, since this rate is due in part to the amount of flanking DNA present in the construct. To make the disruption construct, the entire *CPRI* ORF was replaced with a cassette consisting of the hygromycin phosphotransferase B gene linked to a kanamycin resistance gene (Fig. 4B). We selected 63 hygromycin-resistant primary transformants, and all

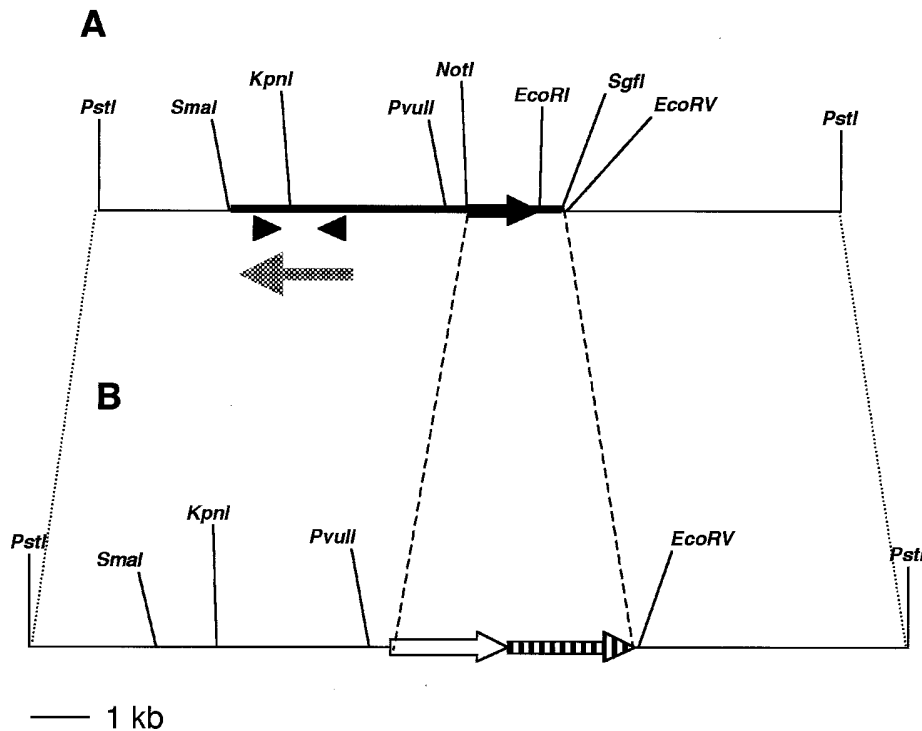


Fig. 4. Partial restriction map of an 8-kb *PstI* subclone containing *CPRI*. **A**, The *CPRI* gene is indicated by the arrow. The heavy line represents the 3.6-kb *SmaI/EcoRV* subclone that was completely sequenced. The second putative gene predicted by the gene finder algorithms is indicated by the dotted arrow beneath the figure. The two arrowheads show the positions of primers that were developed to amplify a genomic fragment of the putative gene for use as a probe in northern blots. The *PvuII* site used to subclone fragments of the 3.6-kb sequence containing *CPRI* or the second putative gene alone is indicated on the figure. **B**, A partial restriction map of the gene knock-out construct made for the deletion experiments. The *CPRI* open reading frame was removed by digestion with *NotI* and *SgfI* and replaced with a cassette containing the selectable hygromycin phosphotransferase gene (striped arrow) linked to a kanamycin resistance gene (white arrow).

of these were analyzed by Southern blot. However, all of these transformants had ectopic integrations rather than homologous gene replacements (data not shown). In contrast, when we used the undisrupted 8-kb subclone containing the *CPRI* gene to transform and complement the REMI mutant strain, homologous recombination occurred in four out of eight transformed strains by a double cross-over event (data not shown).

Transcript analysis by reverse transcription-polymerase chain reaction (RT-PCR).

We performed a RT-PCR using primers that spanned the predicted intron of *CPRI* (Fig. 5). To test whether the integration in the original REMI mutant had occurred within the 3' untranslated region (UTR) of the *CPRI* gene, the primers also spanned the *EcoRI* recognition sequence that was the REMI integration site. We amplified a product of the expected size

from total RNA prepared from a wild-type culture grown in liquid complete medium (data not shown). The amplified product was gel-purified and sequenced to confirm its identity. The sequence of the amplified product was completely consistent with our prediction of the location of the intron and of the location of the *EcoRI* site within the 3' UTR. No product was amplified with these primers from RNA prepared from the mutant strain. We produced a second set of primers that spanned the intron but did not include any of the 3' UTR sequence, and these also amplified the expected product from the wild type (confirmed by sequencing) but still failed to amplify a product from the mutant (data not shown).

Analysis of gene expression by northern blot.

We conducted northern blots using the wild-type *CPRI* cDNA fragment produced by RT-PCR as a probe. RNA was



Fig. 5. Part of the 3.6-kb sequence containing the *CPRI* open reading frame. The predicted amino acid sequence is presented below the nucleotide sequence. Putative transcription start sites and upstream regulatory elements (CAAT boxes and AT-rich sequences) are highlighted in bold. A predicted transmembrane region of the protein is underlined. P1 and P2 are the two primers that were used for the reverse transcription-polymerase chain reaction experiments. The *EcoRI* restriction enzyme recognition sequence (GAATTC) in the 3' untranslated region where the restriction-enzyme mediated insertional integration occurred is highlighted in bold. A putative polyadenylation signal (AATAAT) downstream of the stop codon is also highlighted in bold.

purified from the wild-type strain, the REMI mutant strain, and from the mutant strain that had been ectopically transformed and complemented with the 8-kb *CPR1* subclone. A single transcript was evident in both the wild-type strain and the complemented strain. In the mutant strain, a much smaller quantity of a slightly smaller transcript could be seen (Fig. 8).

Northern blots were also performed using as a probe a PCR product produced by amplifying wild-type genomic DNA with primers corresponding to the second putative gene (Fig. 4A). Two extremely faint signals could be seen on the northern blots, and the intensity and position of these were identical in the wild type, the mutant, and the complemented strain (data not shown).

Southern hybridization.

A Southern hybridization was performed at low stringency, using as a probe the *CPR1* cDNA fragment amplified by RT-PCR. Results indicated that there is at least one other sequence in the genome of *C. graminicola* that is similar to the *CPR1* probe (Fig. 9).

DISCUSSION

Using a random mutagenesis approach, we identified a gene we called *CPR1* that plays an important role in pathogenicity of *C. graminicola* to maize leaves and stalks. The predicted product of the *CPR1* gene is similar to a family of polypeptides that comprise one subunit of the eukaryotic SPC. The SPC is responsible for cleavage of signal peptides from proteins destined for transport through the endoplasmic reticulum (ER) membrane system (Green and Fang 1999). Based on the overall sequence similarity of CPR1 to this family of SPC proteins, we propose that *CPR1* encodes the homologous component of the *C. graminicola* SPC. Additional evidence in support of this hypothesis is the presence of a putative signal anchor sequence at the N-terminus of the CPR1 protein, which is consistent

with ER membrane localization. Furthermore, CPR1 also contains an N-terminal transmembrane domain, conserved in all members of this SPC protein family, that traverses the ER membrane and positions the C-terminal portion of the protein within the ER lumen (Shelness et al. 1993).

Relatively little is known about the role the CPR1 family of proteins plays in the SPC. They do not appear to have direct responsibility for catalytic cleavage of signal peptides, which is attributed to another, much more highly conserved family of polypeptides that includes the yeast protein Sec11p (Green and Fang 1999; VanValkenburgh et al. 1999). Significant sequence similarity among the CPR1 family is limited to three highly conserved regions, but the functional connotation of this is unknown. A site-directed mutagenesis study of Spc3p, the CPR1 homologue in yeast, targeted individual amino acids within two of these conserved regions but could not demonstrate a phenotypic effect for any of the mutations (VanValkenburgh et al. 1999). It is known that Sec11p interacts physically with Spc3p (VanValkenburgh et al. 1999). It is also known that both of these proteins are essential in yeast for signal peptidase function, and disruption of the gene encoding either one is lethal (Fang et al. 1997; Meyer and Hartmann 1997). It appears from our study that deletion of *CPR1* may also be lethal, since we were unable to recover a disruptant among 63 transformants. It seems unlikely that this resulted from an inability to perform homologous recombinations in that region due to some structural feature of the DNA because, when we used virtually the same DNA in complementation experiments, we obtained homologous recombinants half the time. Our northern blots revealed that the disrupted *CPR1* gene in our REMI mutant does produce a very small quantity of *CPR1* transcript. Apparently, this is both sufficient and necessary for nearly normal vegetative growth of the mutant strain. The smaller size of the transcript in the mutant probably results from premature termination somewhere beyond the stop codon within the integrated plasmid sequence. Other, larger bands that are faintly

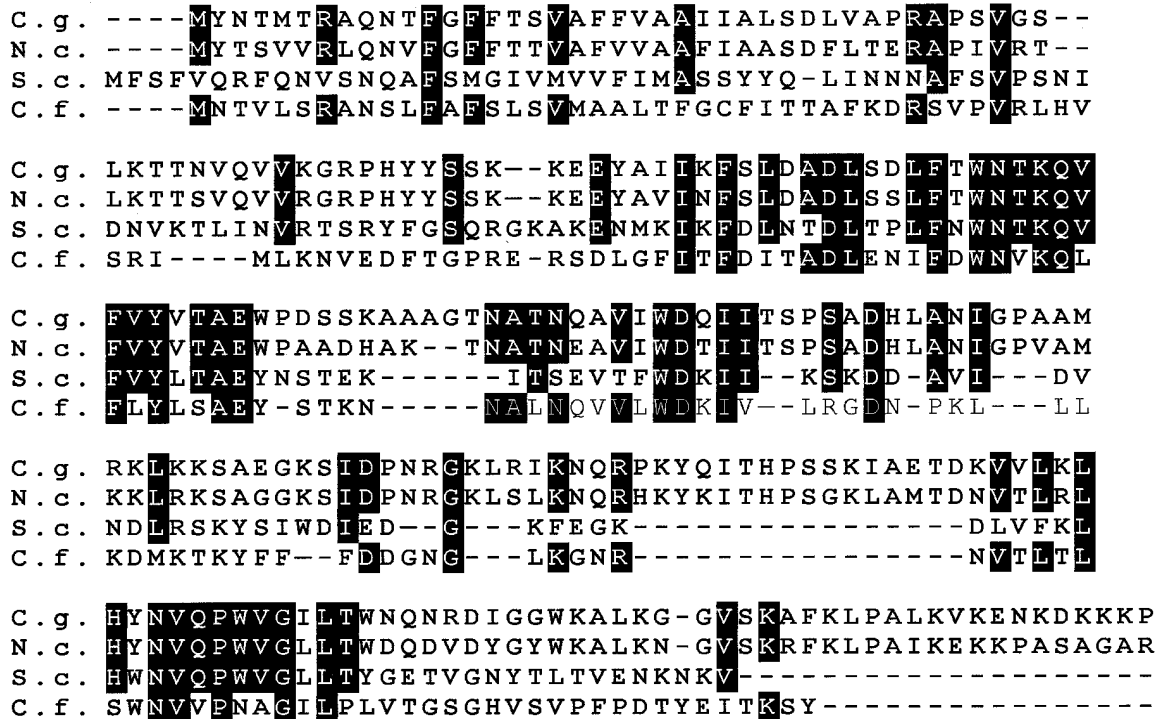


Fig. 6. Multiple sequence alignment of the predicted CPR1 protein from *Colletotrichum graminicola* (C.g.) and the homologous proteins from *Neurospora crassa* (N.c.), *Saccharomyces cerevisiae* (S.c.) (AAB51390), and *Canis familiaris* (C.f.) (A31788). The alignment was made using the CLUSTAL-W multiple alignment program.

visible on the northern blots may result from alternative transcription termination. By altering the sequence of the 3' UTR, we have significantly reduced the quantity of transcript, perhaps as a result of an increase in transcript instability. We assume that the reduction in transcript levels results in a corresponding reduction in protein levels, but this assumption remains to be tested.

Vegetative growth was slightly reduced in the *CPRI* mutant in comparison to the wild type. However, its slower growth rate is unlikely to be primarily responsible for the pathogenicity defect in the *CPRI* mutant, since we obtained other REMI transformants that grew far more slowly (even as little as 37% of the wild-type rate) and were still completely pathogenic to both maize stalks and leaves (M. R. Thon et al., unpublished data). Growth rate of the *CPRI* REMI mutant was restored by transformation with a plasmid containing the *CPRI* gene, and thus, the slower growth appears to be a pleomorphic effect of the *CPRI* mutation. The fact that growth, germination, and development of the mutant are relatively normal in culture, considering the extremely small amount of *CPRI* transcript (and presumably also *CPRI* protein) that it is producing, is rather surprising. Our Southern blots indicate that *C. graminicola* contains a second sequence similar to *CPRI*. It is possible that this sequence represents a second, functional signal peptidase gene, and its product may be able to substitute in vegetative culture for the *CPRI* protein. However, it also appears from our deletion experiments that *CPRI* is essential and so, if there is another gene, it is not completely redundant with *CPRI*. Additionally, this putative second signal peptidase cannot support pathogenic growth.

If *CPRI* encodes a component of the *C. graminicola* SPC, then it seems likely that it is not directly responsible for the pathogenicity defect in the REMI mutant. It is more probable that the nonpathogenic phenotype results from a reduction in the transport of secreted or outer membrane proteins that are directly involved in host colonization, particularly during the necrotrophic phase of the disease cycle. It seems clear from our observations of the mutant *in vivo* that protein transport in this

strain is sufficient to allow the initial, biotrophic phase of the disease cycle to proceed relatively normally. However, transition from the biotrophic to the necrotrophic phase does not seem to occur. One obvious possibility is that the mutant is un-

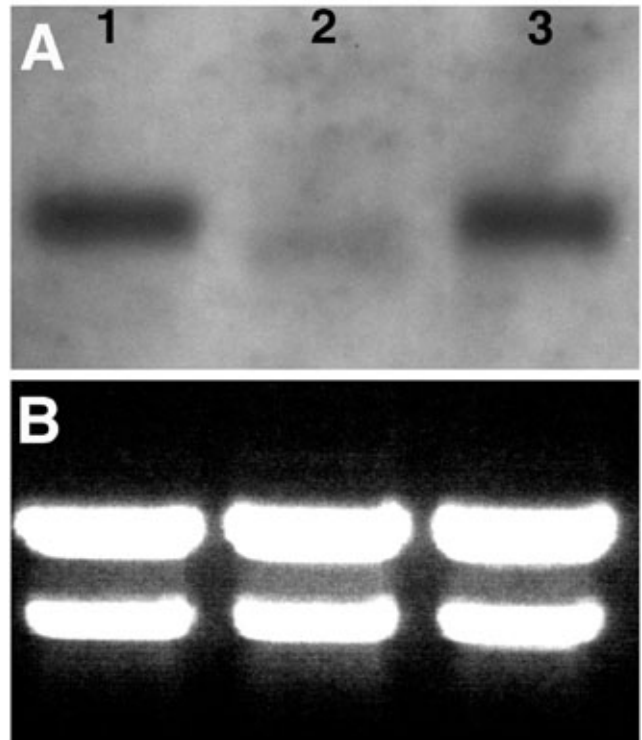


Fig. 8. **A**, Results of a northern blot in which total RNA from the wild-type strain (lane 1), *CPRI* mutant strain (lane 2), and *CPRI* mutant complemented with the 8-kb *Pst*I subclone containing *CPRI* (lane 3) was probed with the *CPRI* cDNA fragment generated by reverse transcription-polymerase chain reaction. **B**, A photograph of the ribosomal RNA bands stained with ethidium to illustrate equal loading.

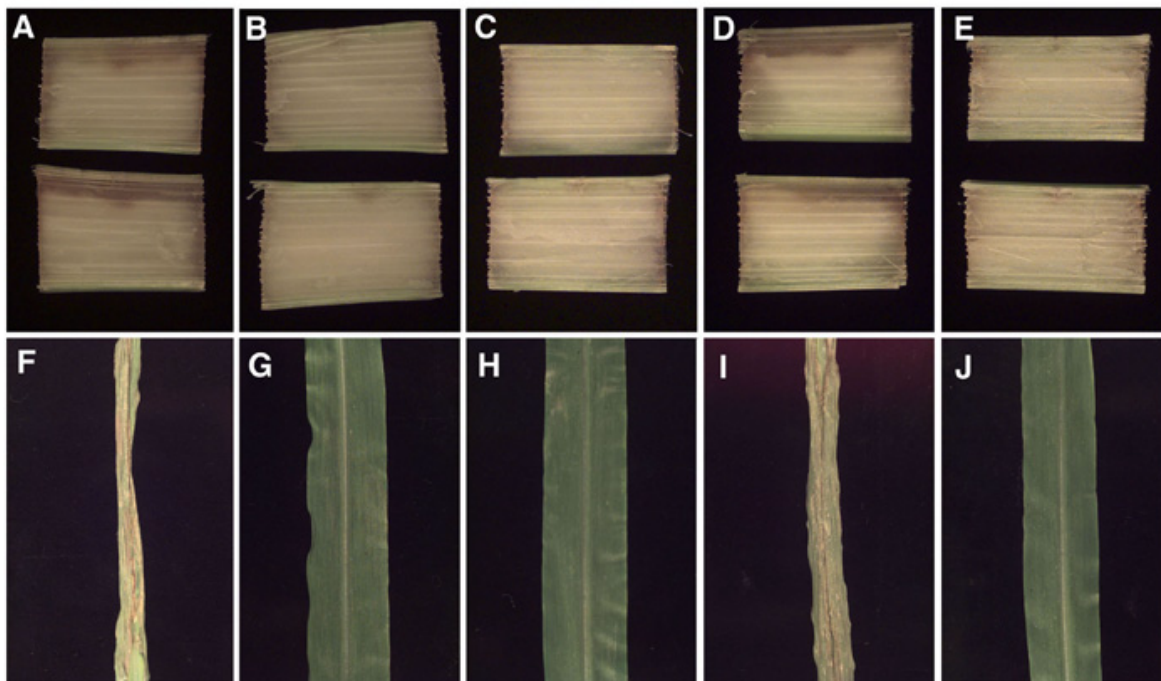


Fig. 7. Results of stalk infection *in vitro* and leaf infection *in vivo* by **A and E**, the wild-type strain; **B and G**, *CPRI* restriction-enzyme mediated insertional (REMI) mutant strain; **C and H**, nonpathogenic *C. sublineolum* control; **D and I**, *CPRI* REMI mutant strain complemented with the 3.6-kb subclone containing the *CPRI* gene; and **E and J**, the *CPRI* mutant strain containing the selectable cotransformation vector alone.

able to secrete required quantities of cell-wall degrading enzymes. Although sufficient for initial host penetration and cell-to-cell growth during biotrophy, there may be a much greater requirement for degradative enzyme secretion during necrotrophic growth. Certainly the virtual lack of cellular integrity in the tissue 72 h after inoculation with the wild-type strain provides ample evidence for the activity of cell-wall degrading enzymes, although these could originate from the host as well as from the pathogen.

The *CPRI* mutant provides us with a unique tool that can be used to study the role of protein transport in pathogenicity. Although it is intuitively obvious that protein transport and secretion are important pathogenicity factors, their precise roles have remained obscure because these are generally essential functions and are, therefore, difficult to study by using a mutagenesis approach. Indeed, our isolation of the *CPRI* mutant was extremely fortuitous, since a complete knock-out mutant would likely have been lethal. The *CPRI* mutant demonstrates that interesting and informative phenotypes beyond simple null mutations are possible with a random mutagenesis approach. In this sense, random mutagenesis offers one important advantage over the directed-knock-out experiments that are increasingly being used as components of functional genomics studies.

MATERIALS AND METHODS

Fungal culture.

C. graminicola strain M1.001 (formerly CgM2; Forgey et al. 1978) was the wild type. The nonpathogenic mutant strain 6-2 was derived by REMI mutagenesis (Thon et al. 2000). The strains were routinely cultured on potato dextrose agar (Difco Laboratories, Detroit, MI, U.S.A.) under continuous fluorescent illumination at 25 to 27°C. Liquid cultures for RNA production were grown in complete medium (Leach et al. 1982) on a rotary shaker at 30°C and 200 rpm. Complete medium was solidified with 15% Bacto-agar (Difco Laboratories) for the radial growth experiments. In those experiments, the minimal medium was complete medium without yeast extract. The medium containing pectin and polygalacturonic acid as carbon sources was complete medium without sucrose or yeast extract and with the addition of 5 g of pectin per liter and 5 g of polygalacturonic acid per liter (Sigma, St. Louis, MO, U.S.A.).

Nucleic acid preparation and Southern and northern hybridizations.

DNA was prepared from all cultures by the miniprep method we have described previously (Thon et al. 2000). Total RNA for RT-PCR and northern blots was prepared using the RNEasy

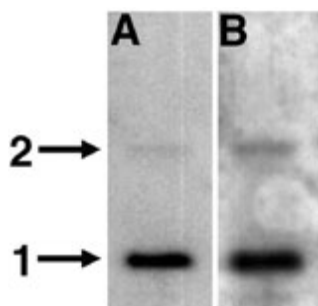


Fig. 9. A, Results of a low stringency Southern blot in which genomic DNA from the wild type was probed with the *CPRI* cDNA generated by reverse transcription-polymerase chain reaction. **B,** Same as A after overdevelopment. Band 1, *CPRI*; and band 2, a second sequence in the genome that is similar to *CPRI*.

kit (Qiagen Inc., Chatsworth, CA, U.S.A.) and the manufacturer's recommended protocols.

For northern hybridizations, 4.5 µg of total RNA was loaded into each lane of an agarose/formaldehyde gel, and electrophoresis at 70 to 80 V continued until the dye had migrated ³/₄ of the length of the gel. For Southern hybridizations, between 0.5 and 1 µg of genomic DNA was loaded into each lane of a 0.8% agarose gel, and electrophoresis at 20 V was continued until the marker dye migrated off the end of the gel. Gels for both northern and Southern hybridizations were blotted onto nylon membranes (Schleicher and Schuell, Keene, NH, U.S.A.), and hybridizations were performed using DIG-labeled DNA probes and the GENIUS nonradioactive EASY-HYB hybridization kit (Boehringer Mannheim, Indianapolis, IN, U.S.A.), according to the manufacturer's protocols. Low stringency Southern blots were performed using a hybridization and wash temperature of 55°C.

Cycle sequencing and RT-PCR.

Sequencing reactions were performed with a PE Applied Biosystems BigDye Terminator Kit and analyzed on a PE Applied Biosystems Model 310 Genetic Analyzer (PE Applied Biosystems, Foster City, CA, U.S.A.). RT-PCR reactions were performed using the ProSTAR Ultra HF RT-PCR system (Stratagene, La Jolla, CA, U.S.A.), according to the manufacturer's instructions.

Fungal transformation.

Production of fungal protoplasts and transformation to hygromycin resistance were done according to a previously described protocol (Thon et al. 2000). Cotransformations were performed by adding a fivefold molar excess of the non-selected plasmid to the hygromycin-selectable plasmid. Transformation to phleomycin resistance used a similar protocol, except that 100 µl of phleomycin (20 mg/ml; Cayla, Toulouse, France) was added to each 40 ml aliquot of protoplasts in regeneration medium just before it was poured into the plates, and hygromycin was not included. The vector containing the phleomycin resistance gene used in these experiments was pAN8.1 (Mattern et al. 1988).

Pathogenicity assays.

In vitro stalk pathogenicity assays and in vivo leaf and stalk pathogenicity assays were performed as described previously (Thon et al. 2000).

Light microscopy.

Leaves were infected for microscopy studies using the cotton swab method described previously (Thon et al. 2000). Tissue samples were collected at 24, 48, or 72 h after inoculation and were fixed and embedded using the protocol of Mims and associates (2001). Embedded tissues were sliced into 1-micron-thick sections, stained with toluidine blue, and observed on a light microscope.

ACKNOWLEDGMENTS

The authors are extremely grateful to our colleague C. Mims of the University of Georgia for preparing the tissue sections that appear in Figure 2 of this manuscript. We appreciate the excellent technical assistance of D. Brown and of R. Green. We thank our colleague C. Poneliet for allowing us to increase our maize inbred lines in his nursery plots. These studies were supported by NRI grant 97-35303-4968 (L. V.) and AREA grant 99-35303-8191 (M. T.) from the U.S. Department of Agriculture, and by a Kentucky Young Scientists Summer Research Program (KYSS) award (J. T.). This is paper number 01-12-154 from the Kentucky Agricultural Experiment Station, published with the permission of the director.

LITERATURE CITED

- Altschul, S. F., Gish, W., Miller, W., Myers, E. W., and Lipman, D. J. 1990. Basic local alignment search tool. *J. Mol. Biol.* 215:403-410.
- Ballance, D. J. 1986. Sequences important for gene expression in filamentous fungi. *Yeast* 2:229-236.
- Bergstrom, G. C., and Nicholson, R. L. 1999. The biology of corn anthracnose: Knowledge to exploit for improved management. *Plant Dis.* 83:596-608.
- Burge, C., and Karlin, S. 1997. Prediction of complete gene structures in human genomic DNA. *J. Mol. Biol.* 268:78-94.
- Fang, H., Mullins, C., and Green, N. 1997. In addition to SEC11, a newly identified gene, SPC3, is essential for signal peptidase activity in the yeast endoplasmic reticulum. *J. Biol. Chem.* 272:13152-13158.
- Forgey, W. M., Blanco, M. H., and Loegering, W. Q. 1978 Differences in pathological capabilities and host specificity of *Colletotrichum graminicola* on *Zea mays*. *Plant Disease Reporter* 62:573-576.
- Green, N., and Fang, H. 1999. Signal peptidase. Pages 2356-2359 in: *Encyclopedia of Molecular Biology*. T. E. Creighton, ed. John Wiley and Sons, New York.
- Gurr, S. J., Unkles, S. E., and Kinghorn, J. R. 1987. The structure and organization of nuclear genes of filamentous fungi. Pages 93-139 in: *Gene Structure in Eukaryotic Microbes*. J. R. Kinghorn, ed. IRL Press, Oxford.
- Kozak, M. 1986. Point mutations define a sequence flanking the AUG initiator codon that modulates translation by eukaryotic ribosomes. *Cell* 44:283-292.
- Leach, J., Lang, B. R., and Yoder, O. C. 1982. Methods for selection of mutants and in vitro culture of *Cochliobolus heterostrophus*. *J. Gen. Microbiol.* 128:1719-1729.
- Mattern, I. E., Punt, P. J., and Van den Hondel, C. A. M. J. J. 1988. A vector of *Aspergillus* transformation conferring phleomycin resistance. *Fungal Genet. Newsl.* 35:25.
- Meyer, H.-A., and Hartmann, E. 1997. The yeast SPC22/23 homolog Spc3p is essential for signal peptidase activity. *J. Biol. Chem.* 272:13159-13164.
- Mims, C. W., Rodriguez-Lothar, C., and Richardson, E. A. 2001. Ultrastructure of the host-pathogen interaction in leaves of *Duchesna indica* infected by the rust fungus *Frommeela mexicana* var. *indicae* as revealed by high pressure freezing. *Can. J. Bot.* 79:49-57.
- Neilsen, H., Engelbrecht, J., Brunak, S., von Heijne, G. 1997. Identification of prokaryotic and eukaryotic signal peptides and prediction of their cleavage sites. *Protein Eng.* 10:1-6.
- Neilsen, H., and Krogh, A. 1998. Prediction of signal peptides and signal anchors by a hidden Markov model. Pages 122-130 in: *Proc. of the Sixth Int. Conf. on Intelligent Systems for Molecular Biology (ISMB Vol. 6)*. J. Glasgow, T. Littlejohn, F. Major, R. Lathrop, D. Sankoff, and C. Sensen, eds. AAAI Press, Menlo Park, CA, U.S.A.
- Shelness, G. S., Lin, L., and Nicchitta, C. V. 1993. Membrane topology and biogenesis of eukaryotic signal peptidase. *J. Biol. Chem.* 268:5201-5208.
- Sonnhammer, E. L. L., von Heijne, G., and Krogh, A. 1998. A hidden Markov model for predicting transmembrane helices in protein sequences. Pages 175-182 in: *Proc. of Sixth Int. Conf. on Intelligent Systems for Molecular Biology (ISMB Vol. 6)*. J. Glasgow, T. Littlejohn, F. Major, R. Lathrop, D. Sankoff, and C. Sensen, eds. AAAI Press, Menlo Park, CA, U.S.A.
- Thon, M. R., Nuckles, E. M., and Vaillancourt, L. J. 2000. Restriction enzyme-mediated integration used to produce pathogenicity mutants of *Colletotrichum graminicola*. *Mol Plant-Microbe Interact.* 13:1356-1365.
- Toman, J., Jr., and White, D. G. 1993. Inheritance of resistance to anthracnose stalk rot of corn. *Phytopathology* 83:981-986.
- VanValkenburgh, C., Chen, X., Mullins, C., Fang, H., and Green, N. 1999. The catalytic mechanism of endoplasmic reticulum signal peptidase appears to be distinct from most eubacterial signal peptidases. *J. Biol. Chem.* 274:11519-11525.
- White, D. G. 1999. *Compendium of Corn Diseases*. 3rd ed. American Phytopathological Society, St. Paul, MN, U.S.A.